ELSEVIER
Journal of Computational and Applied Mathematics 117 (2000) 105–119
JOURNAL OF COMPUTATIONAL AND APPLIED MATHEMATICS
www.elsevier.nl/locate/cam

A posteriori error estimates in finite element acoustic analysis

A. Alonso, A. Dello Russo [*,1], V. Vampa
Departamento de Matemática, Facultad de Ciencias Exactas, Universidad Nacional de La Plata, C. C. 172, 1900 La Plata, Argentina

Received 14 April 1998

Abstract

We present an a posteriori error estimator for the approximations of the acoustic vibration modes obtained by a finite element method which does not present spurious or circulation modes for non zero frequencies. We prove that the proposed estimator is equivalent to the error in the approximation of the eigenvectors up to higher order terms with constants independent of the eigenvalues. Numerical results for some test examples are presented which show the good behavior of the estimator when it is used as local error indicator for adaptive refinement. © 2000 Elsevier Science B.V. All rights reserved.

Keywords: Eigenvalue problem; Finite element method; A posteriori error estimate; Adaptive mesh-refinement technique

1. Introduction

In recent years, considerable interest has been shown in finite element methods to compute the vibration modes of a fluid based on the displacement formulation. One of these methods consists of using the lowest-order triangular Raviart–Thomas elements for fluid variables. It can be proved that this method does not present spurious or circulations modes for nonzero frequencies which are typical of displacement formulation. Also, it exhibits an optimal order of convergence. This methodology was introduced in [3] for fluid–structure interaction problems and good approximations were obtained for compressible and incompressible fluids [6,4].

From the computational point of view, many questions are still open. The necessity of using adequately refined meshes in order to take care of the singularities of the eigenmodes is among the most relevant ones. In this context, a posteriori error estimators play a fundamental role since they are used to know where a given mesh needs to be refined.

* Corresponding author.
[1] Member of Comisión de Investigaciones Científicas de la Provincia de Buenos Aires, Argentina.

0377-0427/00/$ - see front matter
PII: S0377-0427(99)00335-0

There are not many references about a posteriori error estimators for eigenvalue problems. For classical finite element approximations one could cite a paper by Babuška and Rheinboldt [2], which includes as an example a simple one-dimensional eigenvalue problem, and a paper by Verfürth [14], who introduced a general framework to derive error estimators for nonlinear problems and applied it, in particular, to linear eigenvalue problems.

Very recently, an a posteriori error estimator for a mixed finite element approximation of the eigenvalues and the eigenvectors of a second-order elliptic problem was introduced in [9].

In this paper we adapt the techniques presented in [9] to derive an error estimator for the Raviart–Thomas approximations of the acoustic vibration problem. We prove that this error estimator is equivalent to the error up to higher-order terms with constants independent of the eigenvalues and of the mesh size. Finally, we present some numerical experiments which show the good behavior of the estimators when they are used as local error indicators for adaptive refinement.

2. The model problem and its discretization

We consider the problem of determining the vibration modes of an ideal inviscid barotropic fluid contained into a rigid cavity.

Let $\Omega \subset \mathscr{R}^2$ be the domain occupied by the fluid. We assume Ω is a simply connected polygon.

The eigenmodes $\boldsymbol{u} \neq 0$ and the eigenfrequencies $\lambda \geqslant 0$ are the solution of the following spectral problem:

$$\begin{array}{ll} -\nabla(\rho c^2 \operatorname{div} \boldsymbol{u}) = \lambda \rho \boldsymbol{u} & \text{in } \Omega, \\ \boldsymbol{u}.\boldsymbol{n} = 0 & \text{on } \partial\Omega, \end{array} \tag{2.1}$$

where $\boldsymbol{u}$ is the displacement vector in the fluid, ρ is the mass density, c is the acoustic speed in the fluid and $\boldsymbol{n}$ is the outward unit normal vector.

Introducing,

$$p = -\rho c^2 \operatorname{div} \boldsymbol{u}, \tag{2.2}$$

we obtain a mixed formulation of problem (2.1)

$$\begin{array}{ll} \nabla p = \lambda \rho \boldsymbol{u} & \text{in } \Omega, \\ \dfrac{1}{\rho c^2} p + \operatorname{div} \boldsymbol{u} = 0 & \text{in } \Omega, \\ \boldsymbol{u}.\boldsymbol{n} = 0 & \text{on } \partial\Omega. \end{array} \tag{2.3}$$

Let $H_0(\operatorname{div}, \Omega)$: $\{\boldsymbol{v} \in H(\operatorname{div}, \Omega)\colon \boldsymbol{v}.\boldsymbol{n}|_{\partial\Omega} = 0\}$.

The weak formulation of problem (2.3) is then: find $\lambda \geqslant 0$, $\boldsymbol{u} \in H_0(\operatorname{div}, \Omega)$ and $p \in L^2(\Omega)$, with $p \neq 0$, such that

$$\begin{aligned} &-\int_\Omega p \operatorname{div} \boldsymbol{v} = \lambda \rho \int_\Omega \boldsymbol{u}.\boldsymbol{v}, \quad \forall \boldsymbol{v} \in H_0(\operatorname{div}, \Omega), \\ &-\int_\Omega q \operatorname{div} \boldsymbol{u} - \frac{1}{\rho c^2} \int_\Omega pq = 0, \quad \forall q \in L^2(\Omega). \end{aligned} \tag{2.4}$$

In order to ensure well-posedness, we consider the following modified eigenvalue problem: find $\lambda \geqslant 0$, $\boldsymbol{u} \in H_0(\mathrm{div}, \Omega)$ and $p \in L^2(\Omega)$, with $p \neq 0$, such that

$$\begin{aligned} &\rho \int_\Omega \boldsymbol{u}.\boldsymbol{v} - \int_\Omega p \;\mathrm{div}\; \boldsymbol{v} = (\lambda+1)\rho \int_\Omega \boldsymbol{u}.\boldsymbol{v} \quad \forall \boldsymbol{v} \in H_0(\mathrm{div}, \Omega), \\ &-\int_\Omega q \;\mathrm{div}\; \boldsymbol{u} - \frac{1}{\rho c^2}\int_\Omega pq = 0, \qquad \forall q \in L^2(\Omega). \end{aligned} \tag{2.5}$$

Clearly, problem (2.5) has the same eigenvalues and eigenfunctions as problem (2.4) and is a well-posed mixed problem in the sense that the bilinear forms involved satisfy the classical Brezzi's conditions (see [7]).

Let $\{\mathcal{T}_h\}$ be a regular family of triangulations of Ω, and let

$$V_h = \{\boldsymbol{v} \in H_0(\mathrm{div}, \Omega) \colon \boldsymbol{v}|_T \in RT_0(T), \forall T \in \mathcal{T}_h\}$$

and

$$Q_h = \{q \in L^2(\Omega) \colon q|_T \in P_0(T), \forall T \in \mathcal{T}_h\},$$

where $RT_0 = \{\boldsymbol{v} \in P_1(T)^2 \colon \boldsymbol{v}(x,y) = (a+bx, c+by) \colon a,b,c \in R\}$ is the lowest-order Raviart–Thomas space [12].

Then, the mixed finite element approximation of problem (2.5) is: find $\lambda_h \geqslant 0$, $\boldsymbol{u}_h \in V_h$ and $p_h \in Q_h$, with $p_h \neq 0$, such that

$$\begin{aligned} &\rho \int_\Omega \boldsymbol{u}_h.\boldsymbol{v} - \int_\Omega p_h \;\mathrm{div}\; \boldsymbol{v} = (\lambda_h+1)\rho \int_\Omega \boldsymbol{u}_h.\boldsymbol{v}, \quad \forall \boldsymbol{v} \in V_h, \\ &-\int_\Omega q \;\mathrm{div}\; \boldsymbol{u}_h - \frac{1}{\rho c^2}\int_\Omega p_h q = 0, \qquad \forall q \in Q_h. \end{aligned} \tag{2.6}$$

The techniques in [5,13] can be adapted to problem (2.6) in order to prove that its eigenfrequencies converge to those of problem (2.5) and that nonzero frequency spurious modes do not arise in this discretization. More precisely, assume for simplicity that λ is a simple eigenvalue and take $\|p\|_{0,\Omega} = \|p_h\|_{0,\Omega} = 1$, then the following a priori estimates holds:

$$\|\boldsymbol{u} - \boldsymbol{u}_h\|_{0,\Omega} + \|p - p_h\|_{0,\Omega} = \mathrm{O}(h^\alpha), \tag{2.7}$$

$$|\lambda - \lambda_h| = \mathrm{O}(h^{2\alpha}). \tag{2.8}$$

The value of the constant α in (2.7) and (2.8) depends on the regularity of the eigenmodes. In particular, if Ω is a polygonal convex region, the eigenvalues of the discrete problem converge with order $\mathrm{O}(h^2)$.

Now, problem (2.1) can be rewritten in terms of the variable p.

From (2.3) we get

$$\Delta p = \lambda\rho \;\mathrm{div}\; \boldsymbol{u}$$

By using (2.2) and for $\lambda \neq 0$, we obtain the eigenvalue problem

$$\begin{aligned} &-c^2 \Delta p = \lambda p \quad \text{in } \Omega, \\ &\frac{\partial p}{\partial n} = 0 \quad \text{on } \partial\Omega. \end{aligned} \tag{2.9}$$

In [9], an error estimator of the residual type was introduced for the approximation of the eigenvectors of a second-order elliptic problem obtained by the mixed finite element method of Raviart–Thomas of the lowest order. Also in [9], it was proved that this estimator is equivalent to the norm of the error up to higher-order terms with constants that depend on the corresponding eigenvalue.

Following the techniques developed there, we obtain another error estimator. This new estimator contains the same terms than the one presented in [9], (putting $c = 1$ in (2.9)), but they are in a different weighted combination. As we will show in the section below, these weights are very important because they determine the behavior of the estimator when it is used as an error indicator for adaptive mesh refinement.

Moreover, our estimator is equivalent to the norm of the error up to higher-order terms with constants independent of the eigenvalues.

In the next section we adapt the ideas in [9] to our problem.

3. A posteriori error estimator

It can be proved that problem (2.6) is equivalent to a nonconforming approximation of the standard formulation of problem (2.9) (see [1,11]). Let us denote by

$$X_h = \{\phi \in L^2(\Omega)\colon \phi|_T \in P_1(T), \forall T \in \mathscr{T}_h, \phi \text{ is continuous at interior midside points}\},$$

$$B_h = \{b \in H_0^1(\Omega)\colon b|_T \text{ is a cubic polynomial vanishing on } \partial T, \forall T \in \mathscr{T}_h\}$$

$$V_h^{\mathrm{d}} = \{\boldsymbol{v} \in (L^2(\Omega))^2\colon \boldsymbol{v}|_T \in RT_0(T), \forall T \in \mathscr{T}_h\}$$

and

$$W_h = X_h \oplus B_h.$$

Let P and Π be the L^2-projection operators onto Q_h and V_h^{d}, respectively.

Then, it can be proved that problem (2.6) is equivalent to problem

$$\sum_{T\in\mathscr{T}_h} \int_T \Pi(\nabla\varphi_h).\nabla\varphi = \frac{\lambda_h}{c^2}\int_\Omega P\phi_h\varphi, \quad \forall\varphi \in W_h, \tag{3.10}$$

in the sense that they have the same eigenvalues λ_h and the eigenvectors are related by

$$\lambda_h \rho \boldsymbol{u}_h = \Pi(\nabla\phi_h), \tag{3.11}$$

$$p_h = P\phi_h. \tag{3.12}$$

For the eigenvectors of (3.10) the following a priori error estimate holds:

$$\|p - \bar{\phi}_h\|_{0,\Omega} = \mathrm{O}(h^{2\alpha}), \tag{3.13}$$

where $\bar{\phi}_h = \phi_h/\|\phi_h\|_{0,\Omega}$.

The double order for convergence of eigenvectors (3.13) is one of the results presented in [9] and it will allow us to obtain an a posteriori estimator equivalent to the error in H (div)-norm up to higher-order terms.

For each edge l of the triangulation $\mathscr{T}_h$, we define

$$J_l = \begin{cases} [\![\boldsymbol{u}_h.\boldsymbol{t}]\!]_l & \text{if } l \not\subset \partial\Omega, \\ 0 & \text{if } l \subset \partial\Omega, \end{cases}$$

where $\boldsymbol{t}$ is a unit tangent on l in an arbitrary, but fixed, orientation.

For any $T \in \mathscr{T}_h$, we define as a local error estimator

$$\eta_T^2 = \frac{\lambda_h^2}{c^4}|T|\,\|\boldsymbol{u}_h\|_{0,T}^2 + \sum_{l \subset \partial T} |l|\,\|J_l\|_{0,l}^2,$$

where $|T|$ and $|l|$ are the area of T and the length of l, respectively.

Let,

$$\eta^2 = \sum_{T \in \mathscr{T}_h} \eta_T^2.$$

Theorem 3.1. *There exist positive constants C_1 and C_2, depending on the regularity of the mesh but independent of λ, such that*

$$\|\boldsymbol{u} - \boldsymbol{u}_h\|_{H(\mathrm{div},\Omega)} \leqslant C_1\eta + \frac{C_2}{\rho c^2}\|p - \bar{\phi}_h\|_{0,\Omega}. \tag{3.14}$$

Proof. Since $\boldsymbol{u} - \boldsymbol{u}_h \in H(\mathrm{div},\Omega)$, we can decompose it as

$$\boldsymbol{u} - \boldsymbol{u}_h = \nabla s + \mathbf{curl}\,\xi, \tag{3.15}$$

where $s \in H^1(\Omega)$ is a solution of

$$\Delta s = \mathrm{div}(\boldsymbol{u} - \boldsymbol{u}_h) \quad \text{in } \Omega,$$

$$\frac{\partial s}{\partial n} = 0 \quad \text{on } \partial\Omega$$

and $\xi \in H_0^1(\Omega)$.

(In what follows, C will denote a constant independent of h and λ, but not necessarily the same at each occurrence.)

Because of the standard a priori estimate for the Neumann problem (see [10]),

$$\|\nabla s\|_{0,\Omega} \leqslant C\|\mathrm{div}(\boldsymbol{u} - \boldsymbol{u}_h)\|_{0,\Omega}.$$

Now,

$$\|\mathrm{div}(\boldsymbol{u} - \boldsymbol{u}_h)\|_{0,\Omega} = \frac{1}{\rho c^2}\|p - p_h\|_{0,\Omega} \leqslant \frac{1}{\rho c^2}(\|p - \bar{\phi}_h\|_{0,\Omega} + \|\bar{\phi}_h - P\phi_h\|_{0,\Omega}),$$

where we used (3.12) to replace p_h.

Since we have taken $\|p_h\|_{0,\Omega} = 1$, a straightforward computation yields

$$\|\bar{\phi}_h - P\phi_h\|_{0,\Omega} \leqslant 2\|\phi_h - P\phi_h\|_{0,\Omega}.$$

So, we have

$$\|\mathrm{div}(\boldsymbol{u} - \boldsymbol{u}_h)\|_{0,\Omega} \leqslant \frac{1}{\rho c^2}\|p - \bar{\phi}_h\|_{0,\Omega} + \frac{2}{\rho c^2}\|\phi_h - P\phi_h\|_{0,\Omega}. \tag{3.16}$$

Now, it is known that

$$\|\phi_h - P\phi_h\|_{0,T} \leqslant C\|\nabla\phi_h\|_{0,T}|T|^{1/2}.$$

Using (3.11) we can obtain

$$\begin{aligned}\|\phi_h - P\phi_h\|_{0,T} &\leqslant C(\|\nabla\phi_h - \Pi\nabla\phi_h\|_{0,T} + \|\lambda_h\rho\boldsymbol{u}_h\|_{0,T})|T|^{1/2}\\ &\leqslant C(|\nabla\phi_h|_{1,T}|T| + \|\lambda_h\rho\boldsymbol{u}_h\|_{0,T}|T|^{1/2}),\end{aligned} \tag{3.17}$$

where the last inequality follows from standard error estimates for Π.

We are going to prove that the first term on the right-hand side of (3.17) is bounded by the second one.

Let

$$\phi_h = \bar{p}_h + \beta_h$$

with $\bar{p}_h$ piecewise linear and $\beta_h = \sum_{T\in\mathscr{T}_h} c_T b_T$, where $b_T = b|_T$. It is easy to see that

$$|\nabla\phi_h|_{1,T} = |c_T|\,|b_T|_{2,T}.$$

Taking b_T as test function in (3.10), we have

$$\int_T \Pi(\nabla\bar{p}_h).\nabla b_T + \int_T \Pi(\nabla\beta_h).\nabla b_T = \frac{\lambda_h}{c^2}\int_T p_h b_T. \tag{3.18}$$

Because $\nabla\bar{p}_h \in V_h^{\mathrm{d}}$,

$$\Pi(\nabla\bar{p}_h) = \nabla\bar{p}_h$$

and integrating by parts, we obtain

$$\int_T \Pi(\nabla\bar{p}_h).\nabla b_T = \int_T \nabla\bar{p}_h.\nabla b_T = -\int_T \operatorname{div}(\nabla\bar{p}_h)b_T + \int_{\partial T}\nabla\bar{p}_h.\boldsymbol{n}b_T = 0.$$

Now, since

$$\int_T \Pi(\nabla b_T).\nabla b_T = \|\Pi(\nabla b_T)\|_{0,T}^2$$

from (3.18) it follows that

$$\int_T \Pi(\nabla\beta_T).\nabla b_T = c_T\int_T \Pi(\nabla b_T).\nabla b_T = c_T\|\Pi(\nabla b_T)\|_{0,T}^2 = \frac{\lambda_h}{c^2}\int_T p_h b_T$$

and so

$$c_T = \frac{\lambda_h}{c^2}p_h\frac{\int_T b_T}{\|\Pi(\nabla b_T)\|_{0,T}^2}.$$

Under the regularity assumption on the meshes, it can be proved that

$$|c_T| \leqslant C\frac{\lambda_h}{c^2}|p_h|\frac{\|b_T\|_{0,T}}{\|\Pi(\nabla b_T)\|_{0,T}^2}|T|^{1/2} \leqslant C\frac{\lambda_h}{c^2}|p_h|\,|T| \leqslant C\frac{\lambda_h}{c^2}\|p_h\|_{0,T}|T|^{1/2} \tag{3.19}$$

and

$$|b_T|_{2,T} \leqslant C|T|^{-1/2}. \tag{3.20}$$

Combining (3.19) and (3.20), we have

$$|\nabla\phi_h|_{1,T} \leqslant C\frac{\lambda_h}{c^2}\|p_h\|_{0,T} = C\lambda_h\rho\|\text{div}\, \boldsymbol{u}_h\|_{0,T}$$

and using an inverse estimate, we obtain

$$|\nabla\phi_h|_{1,T}|T| \leqslant C\lambda_h\rho\|\boldsymbol{u}_h\|_{0,T}|T|^{1/2}, \tag{3.21}$$

which gives the desired result.

Now, (3.16) together with (3.17) and (3.21) yields

$$\|\nabla s\|_{0,\Omega} \leqslant C\left(\sum_{T\in\mathscr{T}_h}\frac{\lambda_h}{c^2}\|\boldsymbol{u}_h\|_{0,\Omega}|T|^{1/2} + \frac{1}{\rho c^2}\|p - \bar{\phi}_h\|_{0,\Omega}\right). \tag{3.22}$$

Finally, it remains to bound $\|\mathbf{curl}\ \xi\|_{0,\Omega}$.

Let $\xi^I \in H_0^1(\Omega)$ be a continuous piecewise linear approximation of ξ such that

$$\|\xi - \xi^I\|_{0,l} \leqslant C|\xi|_{1,\tilde{T}}|l|^{1/2}, \quad \forall l \subset \partial T, \tag{3.23}$$

where $\tilde{T}$ is the union of the triangles sharing a vertex with T (see [8], for instance).

Since decomposition (3.15) is orthogonal in $\|.\|_{0,\Omega}$ and $\mathbf{curl}\,\xi^I \in V_h$, by using (2.4) and (2.6) we have

$$\|\mathbf{curl}\ \xi\|_{0,\Omega}^2 = -\int_\Omega \boldsymbol{u}_h.\mathbf{curl}(\xi - \xi^I) = -\sum_{T\in\mathscr{T}_h}\int_{\partial T}\boldsymbol{u}_h.\boldsymbol{t}(\xi - \xi^I)$$

$$= -\frac{1}{2}\sum_{T\in\mathscr{T}_h}\sum_{l\subset\partial T}\int_l J_l(\xi - \xi^I).$$

Now, using (3.23) we obtain

$$\|\mathbf{curl}\ \xi\|_{0,\Omega} \leqslant C\sum_{T\in\mathscr{T}_h}\left(\sum_{l\subset\partial T}\|J_l\|_{0,l}|l|^{1/2}\right). \tag{3.24}$$

Therefore, (3.14) follows from (3.16), (3.22) and (3.24). □

In the next theorem we are going to prove that our error estimator gives a local lower bound for the true error in H (div)-norm.

Theorem 3.2. *There exist positive constants C_3 and C_4, depending on the regularity of the mesh but independent of λ, such that*

$$\eta_T \leqslant C_3\|\boldsymbol{u} - \boldsymbol{u}_h\|_{H(\text{div},T^*)} + C_4\|\lambda\boldsymbol{u} - \lambda_h\boldsymbol{u}_h\|_{0,T}\frac{|T|^{1/2}}{c^2}, \tag{3.25}$$

where T^* is the union of the triangles sharing an edge with T.

Proof. Let $T \in \mathscr{T}_h$ and put $\boldsymbol{z} = -v\boldsymbol{u}_h b_T$. Observing that $\boldsymbol{z} \in H_0(\text{div}, \Omega)$, we have

$$\int_T \text{div}\, \boldsymbol{z}\ p_h = -\int_T \boldsymbol{z}.\nabla p_h + \int_{\partial T} p_h\,\boldsymbol{z}.\boldsymbol{n} = 0. \tag{3.26}$$

Combining (2.4) and (2.6) and using (3.26) we may write

$$\int_T (p - p_h)\operatorname{div} z + \int_T \rho(\lambda \boldsymbol{u} - \lambda_h \boldsymbol{u}_h).z = -\lambda_h \int_T \rho \boldsymbol{u}_h.z. \tag{3.27}$$

Choosing $v = (\lambda_h |T| \|\boldsymbol{u}_h\|_{0,T}^2)/(\rho c^4 \int_T |\boldsymbol{u}_h|^2 b_T)$, we have

$$-\lambda_h \rho \int_T \boldsymbol{u}_h.z = \frac{\lambda_h^2}{c^4} \|\boldsymbol{u}_h\|_{0,T}^2 |T| \tag{3.28}$$

and using standard homogeneity arguments, we obtain after some computations

$$\|z\|_{0,T} \leqslant C \frac{\lambda_h}{\rho c^4} \|\boldsymbol{u}_h\|_{0,T} |T|, \tag{3.29}$$

$$|z|_{1,T} \leqslant C \frac{\lambda_h}{\rho c^4} \|\boldsymbol{u}_h\|_{0,T} |T|^{1/2}. \tag{3.30}$$

Thus, (3.27) with (3.28), (3.29) and (3.30) yields

$$\frac{\lambda_h}{c^2} \|\boldsymbol{u}_h\|_{0,T} |T|^{1/2} \leqslant C \left(\|\operatorname{div}(\boldsymbol{u} - \boldsymbol{u}_h)\|_{0,T} + \|\lambda \boldsymbol{u} - \lambda_h \boldsymbol{u}_h\|_{0,T} \frac{|T|^{1/2}}{c^2} \right), \tag{3.31}$$

where we have used that $\operatorname{div}(\boldsymbol{u} - \boldsymbol{u}_h) = (-1/\rho c^2)(p - p_h)$.

To conclude the theorem, it is enough to prove that

$$\|J_l\|_{0,l} |l|^{1/2} \leqslant C \|\boldsymbol{u} - \boldsymbol{u}_h\|_{0,T^*}. \tag{3.32}$$

The proof will not be given here because it is essentially identical to that in [9].

Finally, (3.25) follows from (3.31) and (3.32). □

Remark. It is not difficult to show that the second term appearing on the right-hand side of (3.25) is a higher-order term. In fact, we have

$$\|\lambda \boldsymbol{u} - \lambda_h \boldsymbol{u}_h\|_{0,T} \leqslant |\lambda - \lambda_h| \|\boldsymbol{u}\|_{0,T} + \lambda_h \|\boldsymbol{u} - \boldsymbol{u}_h\|_{0,T}$$

and observing that

$$\|\boldsymbol{u} - \boldsymbol{u}_h\|_{0,T} \leqslant \|\boldsymbol{u} - \boldsymbol{u}_h\|_{H(\operatorname{div},T^*)},$$

it follows that $|T|^{1/2} \|\boldsymbol{u} - \boldsymbol{u}_h\|_{0,T}$ is of higher-order than $\|\boldsymbol{u} - \boldsymbol{u}_h\|_{H(\operatorname{div},T^*)}$. Finally, we can use the a priori estimate (2.8) for the term $|\lambda - \lambda_h|$.

4. Numerical results

In this section we present the results of some numerical computation. We consider the problem of a rigid L-shaped cavity with air inside.

The geometrical data can be seen in Fig. 1.

We have taken the following values of the physical parameters:

$\rho = 1$ kg/m^3,

$c = 340$ m/s.

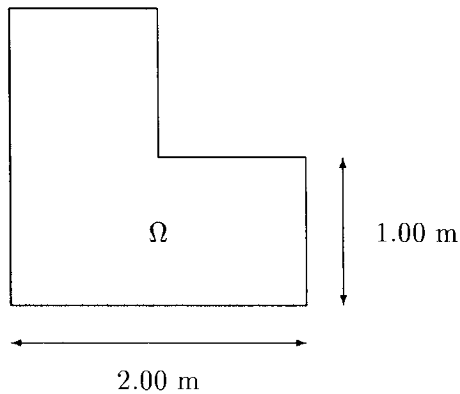

Fig. 1.

Table 1
Eigenfrequencies computed by using uniform refinement

Mode	$N = 5280$	$N = 9344$	$N = 14560$	$N = 20928$	Order	λ_{exact}
F_1	412.293	412.527	412.654	412.733	1.36	413.013
F_2	639.155	639.160	639.162	639.164	1.72	639.167
F_3	1067.682	1067.883	1067.976	1068.027	2.00	1068.141
F_4	1068.093	1068.114	1068.124	1068.129	2.01	1068.142
F_5	1147.241	1147.329	1147.370	1147.392	1.99	1147.442
F_6	1204.868	1205.079	1205.197	1205.272	1.25	1205.566
F_7	1510.938	1510.782	1510.709	1510.670	1.99	1510.580
F_8	1571.465	1572.302	1572.728	1572.978	1.63	1573.700

In Table 1 we present the computed lowest eigenfrequencies for several embedded meshes. We denote by N the number of the unknowns. Because no analytical expression for the eigenvalues is known, we have extrapolated the computed ones to obtain what will be denoted by λ_{exact}. We also used this extrapolation techniques to get an estimation of the order of convergence in powers of $h = \mathrm{O}(1/\sqrt{N})$.

Since Ω has reentrant corners, eigenfunctions with singularities are expected. In these cases, the order of convergence is less than 2 which is the order predicted by the theory for regular eigenfunctions.

Fig. 2 presents some computed eigenmodes. It shows the displacement in the fluid corresponding to the eigenvalues F_1, F_2, F_5 and F_6. Observe the singular behavior of the displacement near the corner in modes F_1 and F_6.

Mode F_2 represents a particular case: although its corresponding displacement field is regular, it converges much slower than regular eigenmodes.

We present below the results obtained with meshes generated by the following adaptive method. The process starts with a uniform triangulation $\mathscr{T}_0$. By using η_T as an error indicator at the element

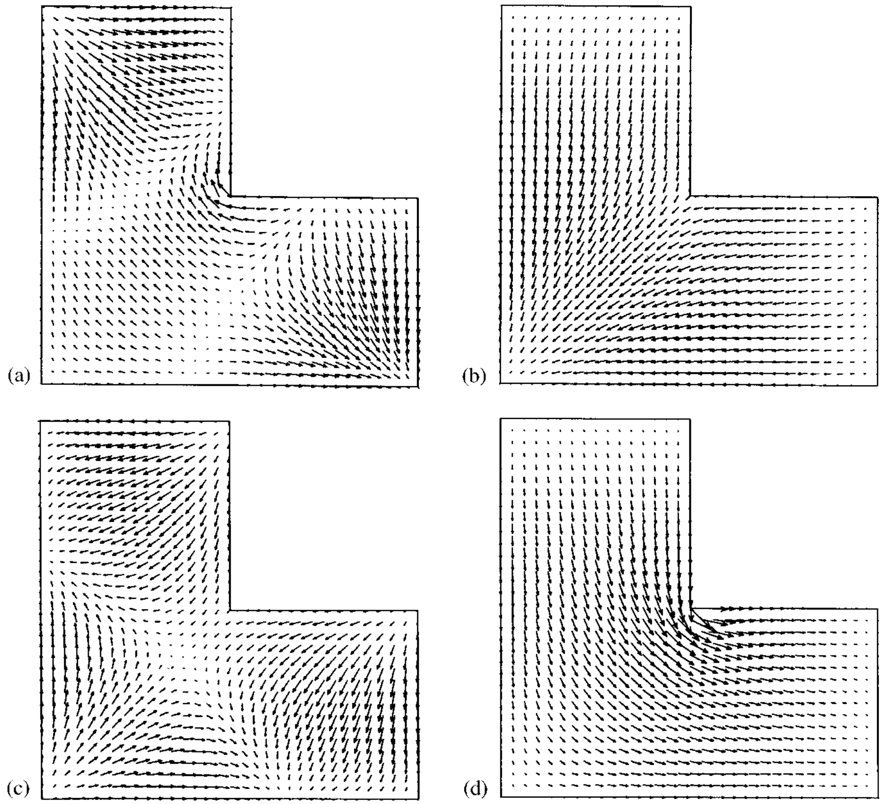

Fig. 2. Fluid displacements in a rigid L-shaped cavity: (a) eigenmode F_1; (b) eigenmode F_2; (c) eigenmode F_5; (d) eigenmode F_6.

T, $\mathscr{T}_{k+1}$ is obtained from $\mathscr{T}_k$ refining all $T \in \mathscr{T}_k$ with

$$\eta_T \geqslant \gamma \max_{T' \in \mathscr{T}_k} \eta_{T'}.$$

In our experiments we have taken $\gamma = 0.5$ and we have started the process from a very coarse mesh.

Tables 2–4 show the results obtained in six steps of the refinement procedure for eigenmodes F_1, F_6 and F_8, respectively. Now, the order of convergence is computed in powers of $1/N$ and it is almost exactly 1 for all these eigenfrequencies. In another words, the optimal order of convergence with respect to the number of nodes was obtained for these singular eigenmodes. It is interesting to observe the significant reduction of the necessary computational effort to obtain a solution with a prescribed accuracy.

Numerical experiments for the regular eigenmodes were also performed. In Tables 5–7 we present the results of these experiments for eigenmodes F_2, F_5 and F_7, respectively.

A not monotone convergence can be observed for mode F_2. This could be a consequence of the particular behavior of this eigenmode already indicated. However, after five steps of the refinement procedure, the error in λ was reduced by 10, approximately.

Table 2
Eigenmode F_1 computed by using adaptive refinement

k	N	λ_h	$\lvert\lambda_{\text{exact}} - \lambda_h\rvert$
0	160	404.489	8.524
1	208	407.793	5.220
2	469	410.879	2.134
3	628	411.676	1.337
4	925	412.039	0.974
5	1752	412.556	0.457
6	2578	412.709	0.304
Order = 1.13			

Table 3
Eigenmode F_6 computed by using adaptive refinement

k	N	λ_h	$\lvert\lambda_{\text{exact}} - \lambda_h\rvert$
0	160	1198.613	6.952
1	431	1199.141	6.425
2	1103	1202.844	2.722
3	1994	1204.271	1.295
4	4097	1204.787	0.778
5	6203	1205.170	0.396
6	10200	1205.328	0.238
Order = 1.04			

Table 4
Eigenmode F_8 computed by using adaptive refinement

k	N	λ_h	$\lvert\lambda_{\text{exact}} - \lambda_h\rvert$
0	160	1526.081	47.619
1	516	1561.311	12.389
2	859	1566.104	7.596
3	2202	1570.848	2.852
4	3251	1571.776	1.923
5	8254	1572.991	0.709
6	11134	1573.235	0.464
Order = 1.07			

With the exception of mode F_2, the obtained results show that the adaptive mesh-refinement procedure does not deteriorate the order of convergence of the regular modes, i.e. these eigenmodes converge with optimal order.

All these results allow us to conclude that our error estimator efficiently detects the regions where the mesh must be refined.

Table 5
Eigenmode F_2 computed by using adaptive refinement

k	N	λ_h	$\lvert\lambda_{\text{exact}} - \lambda_h\rvert$
0	160	639.131	0.0360
1	573	639.117	0.0502
2	1504	639.151	0.0161
3	2433	639.168	0.0014
4	6673	639.160	0.0073
5	9607	639.166	0.0025
Order = –			

Table 6
Eigenmode F_5 computed by using adaptive refinement

k	N	λ_h	$\lvert\lambda_{\text{exact}} - \lambda_h\rvert$
0	160	1140.485	6.957
1	570	1146.060	1.382
2	2050	1147.108	0.334
3	2552	1147.193	0.249
4	8120	1147.344	0.098
5	10331	1147.378	0.064
Order = 1.09			

Table 7
Eigenmode F_7 computed by using adaptive refinement

k	N	λ_h	$\lvert\lambda_{\text{exact}} - \lambda_h\rvert$
0	160	1521.421	10.841
1	586	1514.159	3.580
2	2190	1511.595	1.015
3	8610	1510.777	0.197
4	28208	1510.596	0.017
5	36540	1510.592	0.013
Order = 1.21			

Fig. 3 shows, for eigenmode F_1, the initial triangulation together with three refined triangulations.

We also computed the eigenmodes of the same problem and using the same adaptive mesh-refinement procedure as above but assuming

$$\tilde{\eta}_T^2 = \|\boldsymbol{u}_h\|_{0,T}^2 |T| + \sum_{l \subset \partial T} \|J_l\|_{0,l}^2 |l| \tag{4.33}$$

as the error indicator at the element T. The a posteriori local error estimator (4.33) was introduced in [9].

In Tables 8–10 we show some vibration frequencies computed in this way.

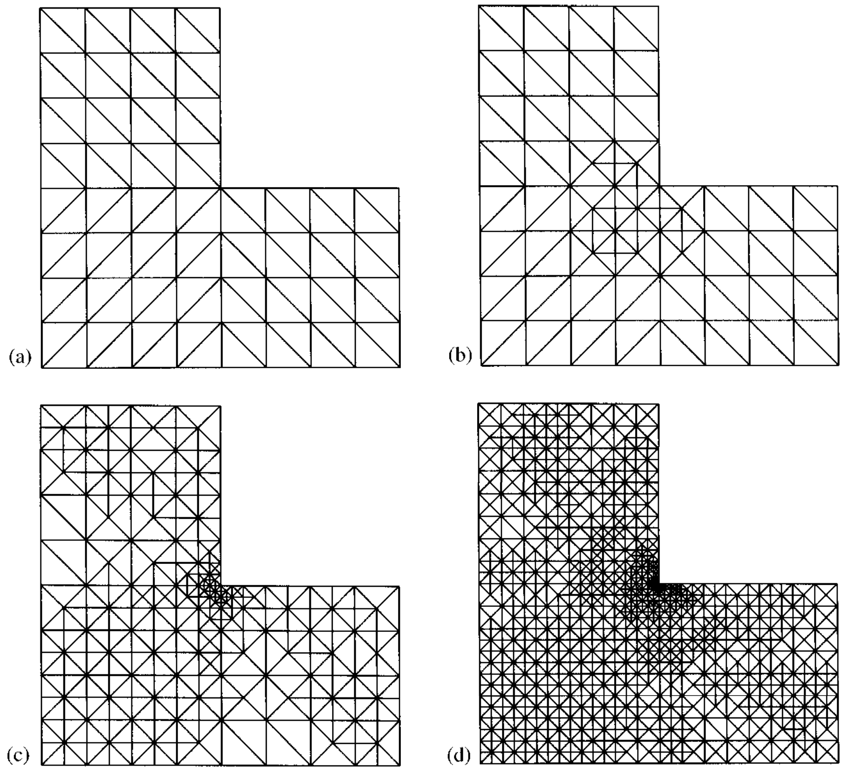

Fig. 3. Initial triangulation and some refined triangulations for Eigenmode F_1: (a) initial triangulation; (b) first refinement step; (c) third refinement step; (d) sixth refinement step.

Table 8
Eigenmode F_2 computed by using adaptive refinement and $\tilde{\eta}_T$

k	N	λ_h	$\lvert\lambda_{\text{exact}} - \lambda_h\rvert$
0	160	639.131	0.036
1	466	640.079	0.912
2	691	639.240	0.073
3	1914	639.332	0.165
4	3273	639.203	0.036
5	7705	639.200	0.033
Order = –			

Now, we observe that modes F_2 and F_8 present a not monotone convergence. Moreover, for mode F_2 the error in λ remains almost the same after five refinements.

Finally, the order of convergence obtained for mode F_7 is not optimal.

Other numerical experiments were performed starting from finer triangulations and using different values of γ. In all these experiments, approximated eigenmodes showing a not monotone convergence or a poor order of convergence were presented.

Table 9
Eigenmode F_7 computed by using adaptive refinement and $\tilde{\eta}_T$

k	N	λ_h	$\|\lambda_{\text{exact}} - \lambda_h\|$
0	160	1521.421	10.841
1	466	1519.211	8.631
2	1298	1519.071	8.492
3	4302	1512.540	1.960
4	8378	1511.770	1.190
5	19426	1510.933	0.354
Order = 0.71			

Table 10
Eigenmode F_8 computed by using adaptive refinement and $\tilde{\eta}_T$

k	N	λ_h	$\|\lambda_{\text{exact}} - \lambda_h\|$
0	160	1526.081	47.619
1	428	1566.524	7.176
2	632	1576.632	2.932
3	1638	1574.554	0.854
4	1717	1574.856	1.156
5	3072	1575.722	2.022
Order = –			

Since the weights of the terms in our estimator are the only differences between this one and $\tilde{\eta}_T$, we can conclude that these weights are very important in order to obtain good local indicators of the error and so, a good performance of an adaptive mesh-refinement process.

Acknowledgements

This work was partially supported by SECYT through grant PIP-292.

References

[1] D.N. Arnold, F. Brezzi, Mixed and nonconforming finite element methods implementation, postprocessing and error estimates, R.A.I.R.O., Modél. Math. Anal. Numer. 19 (1985) 7–32.
[2] I. Babuška, W.C. Rheinboldt, A posteriori error estimators in the finite element method, Int. J. Numer. Meth. Eng. 12 (1978) 1597–1615.
[3] A. Bermúdez, R. Durán, M.A. Muschietti, R. Rodríguez, J. Solomin, Finite element vibration analysis of fluid–solid systems without spurious modes, SIAM J. Numer. Anal. 32 (1995) 1280–1295.
[4] A. Bermúdez, R. Durán, R. Rodríguez, Finite element solution of incompressible fluid-structure vibration problems, Int. J. Numer. Meth. Eng. 40 (1997) 1435–1448.
[5] A. Bermúdez, R. Durán, R. Rodríguez, Finite element analysis of compressible and incompressible fluid–solid systems, Math. Comp. 67 (1998) 111–136.

[6] A. Bermúdez, R. Rodríguez, Finite element computation of the vibration modes of a fluid–solid system, Comput. Methods Appl. Mech. Eng. 119 (1994) 355–370.
[7] F. Brezzi, M. Fortin, Mixed and Hybrid Finite Element Methods, Springer, New York, 1991.
[8] P. Clement, Approximation by finite element functions using local regularization, R.A.I.R.O., Anal. Numer. 9 (1975) 77–84.
[9] R. Durán, L. Gastaldi, C. Padra, A posteriori error estimators for mixed approximations of eigenvalue problems, Math. Models Methods Appl. Sci., to appear.
[10] V. Girault, P.A. Raviart, Finite Element Methods for Navier–Stokes Equations, Springer, Berlin, 1986.
[11] L.D. Marini, An inexpensive method for the evaluation of the solution of the lowest order Raviart–Thomas mixed method, *SIAM* J. Numer. Anal. 22 (1985) 493–496.
[12] P.A. Raviart, J. Thomas, A mixed finite element method for second order elliptic problems, Mathematical aspects of the Finite Elements Method, Lecture Notes in Math., vol. 606, Springer, New York, 1977, 292–315.
[13] R. Rodríguez, J. Solomin, The order of convergence of eigenfrequencies in finite element approximations of fluid structure interaction problems, Math. Comp. 65 (1996) 1463–1475.
[14] R. Verfürth, A posteriori error estimates for nonlinear problems, Math. Comp. 62 (1994) 445–475.